17th World Conference on Earthquake Engineering, 17WCEE
Sendai, Japan - September 13th to 18th 2020

COMPARING DIFFERENT METHODDS TO IDENTIFY STIFFNESS DEGREDATION FOR PINCHED HYSTERETIC STRUCTURES

M. Rabiepour[(1)], C. Zhou[(2)], J.G. Chase[(3)] , G.W. Rodgers[(4)]

[(1)] *PhD candidate, University of Canterbury, mohammad.rabiepour@pg.canterbury.ac.nz*
[(2)] *Post-doctoral Fellow, University of Canterbury, cong.zhou@canterbury.ac.nz*
[(3)] *Distinguished Professor, University of Canterbury, geoff.chase@canterbury.ac.nz*
[(4)] *Professor, University of Canterbury, geoff.rodgers@canterbury.ac.nz*

Abstract

Increasing urbanisation has magnified seismic risk in seismic zones. Rapid and accurate structural health monitoring (SHM) provides significant benefits of assessing damage state, safety in re-occupancy, and thus optimizing decision-making for mitigation and recovery. Many SHM methods have shown their ability to track the change of nonlinear stiffness for damage identification in civil engineering. However, SHM and damage identification for pinched hysteretic systems can be problematic and subjective due to their highly nonlinear and time-varying behavior when damaged. This work compares the efficiency and robustness of a proven hysteresis loop analysis (HLA) method and 7 other SHM methods in identifying stiffness degradation for the pinched hysteretic behaviors, commonly observed in reinforced concrete structures.

The performance of the 8 compared SHM methods are tested using a simulated 6-story numerical structure with pinching, yielding and degrading nonlinear behaviors, where the exact values are known in the presence of both noise-free and 10% root mean square (RMS) noise. Stiffness identification across two major earthquakes are conducted to compare the consistency and accuracy of all the 8 methods. All the 8 methods show a high accuracy of the identified stiffness changes with the average error of 0.4% across all 6 stories and 2 earthquakes in the noise-free case. The average identification error for HLA, CSW and MTD methods are still within 3% in the presence of 10% added noise, while other methods show significant errors of 10.5% with standard deviation (SD) of 13.6%.

Robustness to the measurement sampling rate is also investigated over 50, 100, 250, 500 and 1000Hz. Results show a significant drop of the identification accuracy for 7 of the 8 methods when the sampling rate decrease from 100Hz to 50Hz. However, the identification error for HLA is very robust with the mean error of 0.8% and SD of 0.5% at the sampling rate of 50Hz. The overall results clearly show the robustness, accuracy and automation of HLA over 7 other SHM methods in identifying nonlinear stiffness over multiple events, while other SHM methods may require a more skilled engineering analysis and input to improve its accuracy in the real application.

Keywords: structural health monitoring; SHM; Hysteresis loop analysis; damage identification; pinched hysteresis

1. Introduction

The primary purpose of structural health monitoring (SHM) methods is detecting the presence, location, and the severity of damage after major external loads [1]. SHM techniques fall into model-based and model-free methods [2]. In model-based methods, a computer model of the real structure is identified by comparing a simulated model and measured responses (e.g. [3-9]). Model-free methods depend only on the measured responses by sensors (e.g. [9-16]). The lack of trusted, accurate SHM methods led to significant disagreements about the level of damage and remaining lifetime of several structures in Christchurch, New Zealand after the events of 2010-2011, delaying repair and recovery [17].

Model-based methods can successfully assess damage when the adopted baseline model contains the observed dynamics of the real structure. However, there is always some uncertainty in selecting a baseline model and its dynamics, particularly for nonlinear cases. Any mismatch increases the risk of incorrect damage estimation for model-based methods, limiting their ability [9]. In addition, most model-based and many model-free methods require human input to guide identification, limiting applicability after an event [15].

Reconstructed hysteresis loops have been already used as visual and quantitative indices for damage assessment [18-20]. Lately, a multiple linear regression approach has accurately identified linear and nonlinear structural stiffness from force-deformation loops across multiple events with inter-event consistency not displayed by other methods, which often does not even consider this consistency between events [10, 11, 14, 21]. This hysteresis loop analysis (HLA) method is fully automated, unlike many SHM methods, and has been validated on full-scale and test structures [9, 12, 14, 16].

This study compares the capability of HLA to a wide range of different SHM methods for identifying the evolution of elastic stiffness for a numerical 6-story building with highly nonlinear pinching behavior under the September 2010 and February 2011 Christchurch earthquakes. HLA is compared to methods, including: the model-based Simple Adaptive Control Damage Detection (SACDD) [22], and the model-free Multivariate Adaptive Regression Splines (MARS) [23-25] and some Piecewise Linear Representation (PLR) based [26, 27] methods. The comparisons presented are thus across leading recent methods, not previously examined, and focusing on model-free methods given their ability to capture highly nonlinear behavior. Robustness and accuracy are assessed across different sampling rates, and in the presence of noise.

2. SHM methods

2.1 Numerical model

Fig. 1 shows the 6-story numerical structure with highly nonlinear pinching behavior simulated by a slip-lock Baber-Noori model [28, 29]. Table 1 provides the mechanical properties.

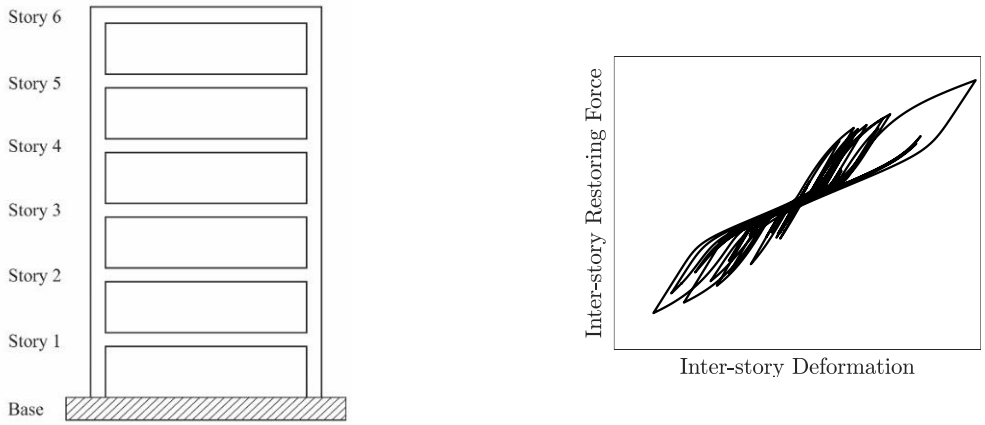

Fig. 1 – Schematic images depicting numerical building and Baber-Noori pinched hysteretic model.

Table 1 – Mechanical properties of the numerical structure.

Story	1	2	3	4	5	6
Mass [kg]	200	250	250	275	285	285
Initial stiffness [KN/m]	450	350	300	400	500	600
Damping ratio [%]	5% for the first two modes					
dy [m]	0.010	0.015	0.015	0.010	0.005	0.002

The dynamic equation of motion for the structure under a seismic excitation can be formulated:

$$F(t) = -MI\ddot{x}_g(t) - M\ddot{X}(t) - C\dot{X}(t) \quad (1)$$

where M and C are the mass and damping matrices, $\dot{X}$ and $\ddot{X}$ are vectors of structural velocity and acceleration, and $\ddot{x}_g$ is the input seismic acceleration. $F(t)$ is the nonlinear restoring force vector, which is decoupled to the inter-story restoring force, $f(t)$, for each degree of freedom/floor, i:

$$f_i(t) = \sum_{j=i}^{nstory} F_j(t) \quad (2)$$

where $nstory$ is the number of stories, and $f(t)$ is defined [28, 29] :

$$f(t) = \alpha K_0 x + (1-\alpha)K_0 z \quad (3)$$

where K_0 and α are the initial elastic stiffness and post-yielding ratio, respectively. The relationship between the inter-story-displacement, x, and hysteretic displacement, z, can be obtained for each story [28-30]:

$$\frac{\dot{z}}{\dot{x}} = h(z) \times \frac{A - \nu(\beta sgn(\dot{x}z) + \gamma)|z|^n}{\eta} \quad (4)$$

where A, β, n and γ are the dimensionless shape parameters of hysteretic loops, $sign(\dot{x}z)$ is the signum function of the product of $\dot{x}$ and z. The parameters η and ν are the stiffness and strength degradation functions:

$$\eta(t) = 1 + \delta_\eta \varepsilon(t) \quad (5)$$

$$\upsilon(t) = 1 + \delta_\upsilon \varepsilon(t) \quad (6)$$

$$\varepsilon(t) = (1-\alpha)\frac{K_e}{m}\int_0^t z(\tau)\dot{x}(t)d\tau \quad (7)$$

where $\varepsilon(t)$ is the total dissipated energy, and the constants δ_η and δ_υ determine the rate of strength and stifness degradation. The term $h(z)$ in Equation (4) is the pinching function, defined:

$$h(z) = 1 - \xi_1 e^{-\left(\frac{zsign(\dot{x}) - qz_u}{\xi_2}\right)^2} \quad (8)$$

where the pinching initiation parameter, q, is a constant, $sign(\dot{x})$ is the signum function of $\dot{x}$, and the ultimate value of z, given by z_u, is defined:

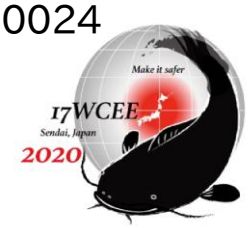

$$z_u(t) = \sqrt[n]{\frac{1}{\upsilon(\beta+\gamma)}} \tag{9}$$

$$\xi_1(t) = \xi_0\left(1 - e^{-p\varepsilon(t)}\right) \tag{10}$$

$$\xi_2(t) = \left(\psi + \delta_\psi \varepsilon\right) \times (\lambda + \xi_1) \tag{11}$$

where ξ_0 is the measure of total slip, p controls the pinching slope, ψ is a constant contributing to the pinching magnitude, δ_ψ is a constant controlling the pinching rate, and λ is a small constant controlling the variation of parameters ξ_1 and ξ_2 [30]. The constant shape parameters are defined: $A = 1$, $\beta = 0.5$, $\gamma = 0.5$, $\nu = 1$ and $n = 2$ [31]. The other Bouc-Wen-Baber-Noori (BWBN) model parameters are summarised in Table 2.

Table 2 – BWBN model parameters for the numerical structure.

Story	α	p	q	λ	ψ	ξ_0	δ_ψ	δ_η	δ_υ
1 - 5	0.2	0.2	0.01	0.05	0.1	0.95	0.001	0.001	0.001
6	0.2	0.2	0.01	0.01	0.1	0.95	0.005	0.001	0.001

The instantaneous tangent stiffness, $K(t)$, can be obtained by differentiating Equation (3) for the restoring force, $f(t)$, with respect to x yielding:

$$K(t) = \frac{df}{dx} = \alpha K_0 + (1-\alpha)K_0 \frac{dz}{dx} \tag{12}$$

Substituting Equation (4), noting $\frac{\dot{z}}{\dot{x}} = \frac{\frac{dz}{dt}}{\frac{dx}{dt}} = \frac{dz}{dx}$, into Equation (12) yields:

$$K(t) = \frac{df}{dx} = \alpha K_0 + (1-\alpha)K_0 h(z) \times \frac{A - \nu(\beta sgn(\dot{x}z) + \gamma)|z|^n}{\eta} \tag{13}$$

The maximum value z_{max} can be found by setting Equation (4) to zero, yielding:

$$z_{max}(t) = \sqrt[n]{\frac{1}{(\beta+\gamma)}} \tag{14}$$

where z_{max} represents the start of purely plastic deformation, and is equal to the yield displacement d_y ($z_{max} = d_y$). Thus, the Equation (13) can be rewritten, considering these values of the shape parameters:

$$K(t) = \frac{df}{dx} = \alpha K_0 + (1-\alpha)K_0 h(z) \times \frac{1 - 0.5\,\upsilon(sgn(\dot{x}z) + 1)\left|\frac{z}{d_y}\right|^n}{\eta} \tag{15}$$

The elastic stiffness, $K_e(t)$, can be estimated by setting $h(z) = 1$ and $z = 0$ in Equation (15) [30]:

$$K_e(t) = \alpha K_0 + (1-\alpha)K_0 \frac{1}{\eta} \tag{16}$$

2.2 Input events and comparison points

The 6-story numerical structure is subjected to two successive earthquakes shown in Fig. 2. All four major events in the Christchurch earthquake series of 2010-11 were followed within 40-180 minutes by an aftershock of similar magnitude [32, 33]. This comparison also tests method robustness across events.

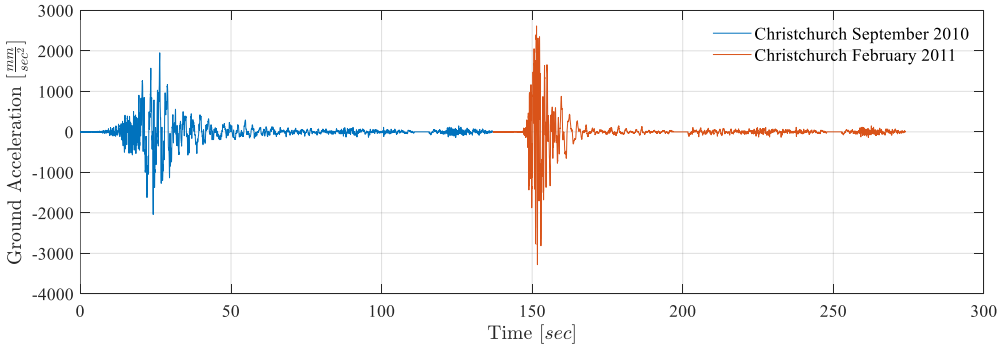

Fig. 2 – Christchurch earthquakes of September 2010 and February 2011.

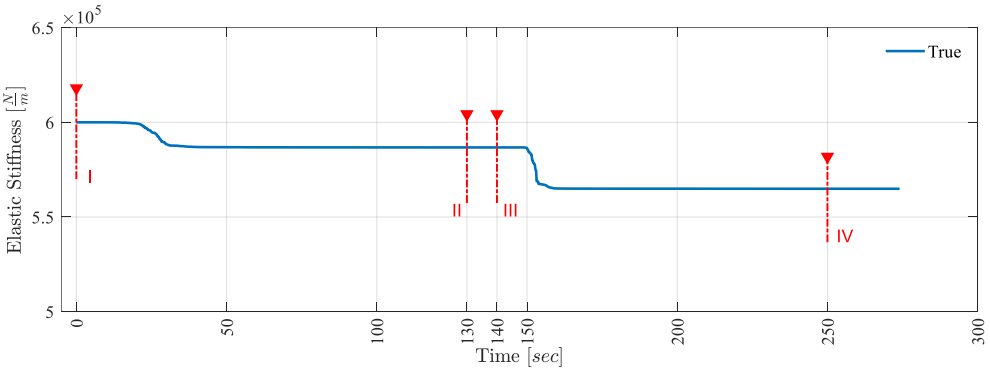

Fig. 3 – Four stages for comparing elastic stifnesses evolution over the two earthquakes.

In particular, to compare SHM methods, the estimated elastic stiffness is compared with the true values at four specific stages defined in Fig. 3. Stages I and III assess initial estimates at the beginning of two major events. Stages II and III assess robustness and accuracy across events. Finally, Stages II and IV assess accuracy over a single major event.

2.3 HLA method

The model-free, mechanics-relevant HLA SHM method is given in detail in [11, 12]. HLA uses regression and a hypothesis test to assess linear and plastic stiffness evolution over time from measured structural responses. The reconstructed hysteresis loop displays the structural load-deformation relationship changing with time due to structural damage. Hence, structural stiffness degradation can be identified from the significant half cycles. HLA is computationally straightforward and wholly automated, with no human input required. Therefore, SHM results can be available immediately after an earthquake or any other event [9, 11, 12, 14].

2.4 SACDD method

SACDD method was proposed for detecting damage in a bilinear chain-like building. It is a model-based method using Simple Adaptive Control (SAC) to estimate restoring forces arising from inter-story stiffness. The input is structural accelerations, and the outputs are inter-story displacements and restoring forces, which can be used to reconstruct responses and time-varying stiffnesses [22].

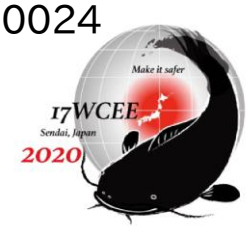

2.5 MARS method

MARS is a model-free regression method, which does make no assumptions regarding the relationship between independent and dependent variables. Instead, segments are derived directly from data in regression process. Thus, MARS is an automated SHM method with continuous models and derivatives [23, 24]. In this paper, the earth package written in RStudio for the MARS algorithm is employed [34].

2.6 PLR-based methods

Piecewise Linear Representation (PLR) techniques are model-free methods, where a half cycle, of length N, is approximated by K linear segments whose slopes represent stiffness [27]. Most PLR algorithms can be classified into one of the three main categories [26]: 1- Sliding Window (SW), 2- Top-Down (TD) and 3- Bottom-Up (BU). The pseudocodes for these algorithms are available in [26]. This paper includes modified versions of SW and TD methods called 4- Constrained sliding Window (CSW) and 5- Modified Top-down (MTD), respectively.

Although PLR-based methods work relatively well on smooth and noise-free half-cycles, they can fragment, especially for small half-cycles, in the presence of noise and need one or more user-specified thresholds to be tuned [26, 27]. Thus, PLR-based algorithm results can be sensitive to thresholds, and cannot be readily automated.

2.6.1 The SW method

The SW method is attractive for its simplicity. In this method, the length of a linear segment increases until the regression error exceeds a user specified bound. This process repeats with the next sample not included in the newly fitted segment [26]. The standard error, SE, is the regression process error with a threshold of $SE = 10$ in this work. PLR utilised in SW (BU and TD as well) can produce a disjointed model, depending on the residual error threshold chosen.

2.6.2 The CSW method

In this method, the first point of the first linear segment is $(0,0)$, from which the slope of the best line fit to the data points creates the first linear segment. For the second segment, the line is constrained to cross the last point of the previous fitted segment. This process repeats for the next segments until the half-cycle reconstruction is complete. This modification leads to a smoother model. Like the SW method, the standard error $SE = 10$ is the threshold for terminating the regression process.

2.6.3 The BU method

This algorithm begins from the tiniest possible segments. The algorithm then iteratively merges adjacent segments until a stopping criteria is met [26]. The terminating criteria is a threshold of $SE = 10$.

2.6.4 The TD method

In this method, a half-cycle is recursively divided into left and right segments until a stopping criteria is met. This algorithm splits the half-cycle where the standard error is a minimum. Both segments are then checked to see if the standard error is less than the defined threshold. If not, the TD algorithm recursively keeps splitting the subsequences until all created segments have a standard error below the chosen threshold of $SE = 10$ [26].

2.6.4 The MTD method

The user-specified threshold has significant impact on PLR-based method performance. The threshold value is selected by trial and error, and is not necessarily optimal for all methods and situations [26, 27]. In this paper, the MTD method is proposed to address this issue.

In the MTD method, each half-cycle is checked to see if it can be represented just by a single linear segment or not. If the R-squared R^2 value of this linear segment is above a user selected minimum value, it can be modelled by one segment. Otherwise, the half-cycle must be further divided. In this study, the R-squared threshold is $R^2 = 0.99$ for noise-free conditions and $R^2 = 0.95$ for noisy cases. These values usually remain unchanged and avoid overfitting.

Since structural hysteresis loops have a range of known fundamental patterns, the maximum number of breakpoints can be estimated as $(7 = 2^3 - 1)$ for half-cycles with pinched nonlinear behavior. The best locations of these breakpoints are obtained by the recursive approach employed in the TD algorithm. Usually, larger half-cycles need more linear segments (or breakpoints) for better approximation, while the smaller ones need fewer segments or even only one. Therefore, extra breakpoints must be pruned to prevent overfitting. For pruning, small segments are merged with adjacent segments, based on reducing standard error. In this research, the minimum length of the segments is limited to 3 samples.

2.7 Analyses

The robustness and accuracy of these SHM methods to sampling rates and sensor noise is investigated separately. To investigate the sampling rate effect, measured accelerations are assumed to be noise-free and measured at the rates of: 1000, 500, 250, 100, and 50 Hz. To assess robustness to noise, 10% root mean square (RMS) noise is added to simulated measurements sampled at 250 Hz [15]. Because of the random nature of noise, each method is run 20 times and the average results are reported in a Monte Carlo approach similar to [15, 21, 35]. Accuracy of methods is assessed at the Stages I-IV depicted in Fig. 3.

3. Results and Discussions

3.1 Sampling rate

Table 3 shows mean value of the absolute error over all 6 stories in identifying elastic stiffness for each method at different sampling rates without noise. The highest mean errors are at a sampling rate of 50 Hz. HLA, BU, TD, and MTD mean errors are less than 1% for all sampling rates. MARS and CSW mean error reaches this level over 100 Hz, whereas SW needs 250 Hz to reach this precision.

Table 4 shows the maximum absolute error over all 6 stories, which more clearly presents the weakness of different methods. Excluding HLA and MTD methods, the maximum errors for all methods are above 5% at 50 Hz. Over 100 Hz, sampling rate impact on the maximum error of the HLA, MARS, TD, and MTD methods is negligible. HLA error is consistently low over all sampling rates.

Table 3 – Mean absolute error and SD for elastic stiffness over all 6 stories for each method (Noise=0); reported in percent.

	50 Hz		**100 Hz**		**250 Hz**		**500 Hz**		**1000 Hz**	
	Mean	**SD**	**Mean**	**SD**	**Mean**	**SD**	**Mean**	**SD**	**Mean**	**SD**
SACDD	Failed	Failed	Failed	Failed	Failed	Failed	0.16	0.22	0.20	0.26
MARS	2.70	4.67	0.54	0.78	0.65	0.92	0.65	0.89	0.51	0.73
SW	3.64	3.56	1.21	0.97	0.76	1.13	0.62	0.63	0.46	0.68
CSW	1.36	1.62	0.61	0.80	0.57	0.93	0.33	0.31	0.36	0.30
BU	0.55	0.48	0.39	0.51	0.34	0.29	0.32	0.44	0.32	0.39
TD	0.66	1.01	0.44	0.39	0.40	0.35	0.35	0.29	0.34	0.29
MTD	0.66	0.80	0.36	0.41	0.31	0.34	0.27	0.30	0.39	0.42
HLA	0.81	0.47	0.66	0.42	0.62	0.37	0.61	0.37	0.72	0.51

Table 4 – Maximum absolute error for elastic stiffness over all 6 stories for each method (Noise=0) ; reported in percent.

	50 Hz	100 Hz	250 Hz	500 Hz	1000 Hz
SACDD	Failed	Failed	Failed	0.71	1.04
MARS	20.75	2.54	2.78	2.41	2.23
SW	11.26	2.88	5.40	2.10	3.17
CSW	7.54	2.72	4.51	0.95	0.95
BU	5.93	2.28	1.03	2.10	1.30
TD	5.04	1.26	1.07	0.88	0.86
MTD	3.26	1.30	1.30	1.01	1.42
HLA	2.08	1.70	1.85	1.80	2.02

The model-based SACDD failed to converge in estimating structural elastic stiffness for the sampling rates below 500 Hz. This failure is mainly because of the control algorithm used in the construction of SACDD. Thus, SACDD, as a model-based SHM approach, is the least robust method to sampling rate.

The results show the modifications applied to SW and TD in this paper (the CSW and MTD methods) enhanced their performance, as seen in Table 4. In particular, at 50 Hz, while the maximum errors of SW and TD are 11.26% and 5.04%, those of CSW and MTD are 7.54% and 3.26%, respectively. However, this improvement is not sufficient to outperform HLA.

3.2 Sensor noise

Table 5 compares methods with 10% added RMS noise and without noise at a realistic to low sampling rate of 250 Hz. As expected, noise diminishes the accuracy of all methods. Again, SACDD failed to converge with 10% added noise at 250 Hz. TD is the least robust method to noise with the maximum error of 49.72% with noise. However, the modified version of TD, MTD, works better in noisy conditions. Excluding HLA, all other methods have maximum errors higher than 10% with noise, which makes them unreliable. The mean error of HLA only increased 1.09% to 1.71% by adding 10% noise, with a 3.90% maximum error. Therefore, HLA is highly robust to sensor noise and better than the other methods presented here in estimating elastic stiffnesses in the presence of noise.

Table 5 – Maximum and mean absolute errors for elastic stiffness over all 6 stories for each method (Noise=0 and 10% Sampling rate = 250 Hz); reported in percent.

	250 Hz					
	0 %			10 %		
	Mean	Max	SD	Mean	Max	SD
SADD	Failed	Failed	Failed	Failed	Failed	Failed
MARS	0.65	2.78	0.92	4.08	16.57	3.96
SW	0.76	5.40	1.13	4.80	13.29	4.00
CSW	0.57	4.51	0.93	2.99	13.76	3.28
BU	0.34	1.03	0.29	4.75	19.74	4.46
TD	0.40	1.07	0.35	10.52	49.72	13.63
MTD	0.31	1.30%	0.34	2.92	10.51	2.54
HLA	0.62	1.8	0.37	1.71	3.90	1.10

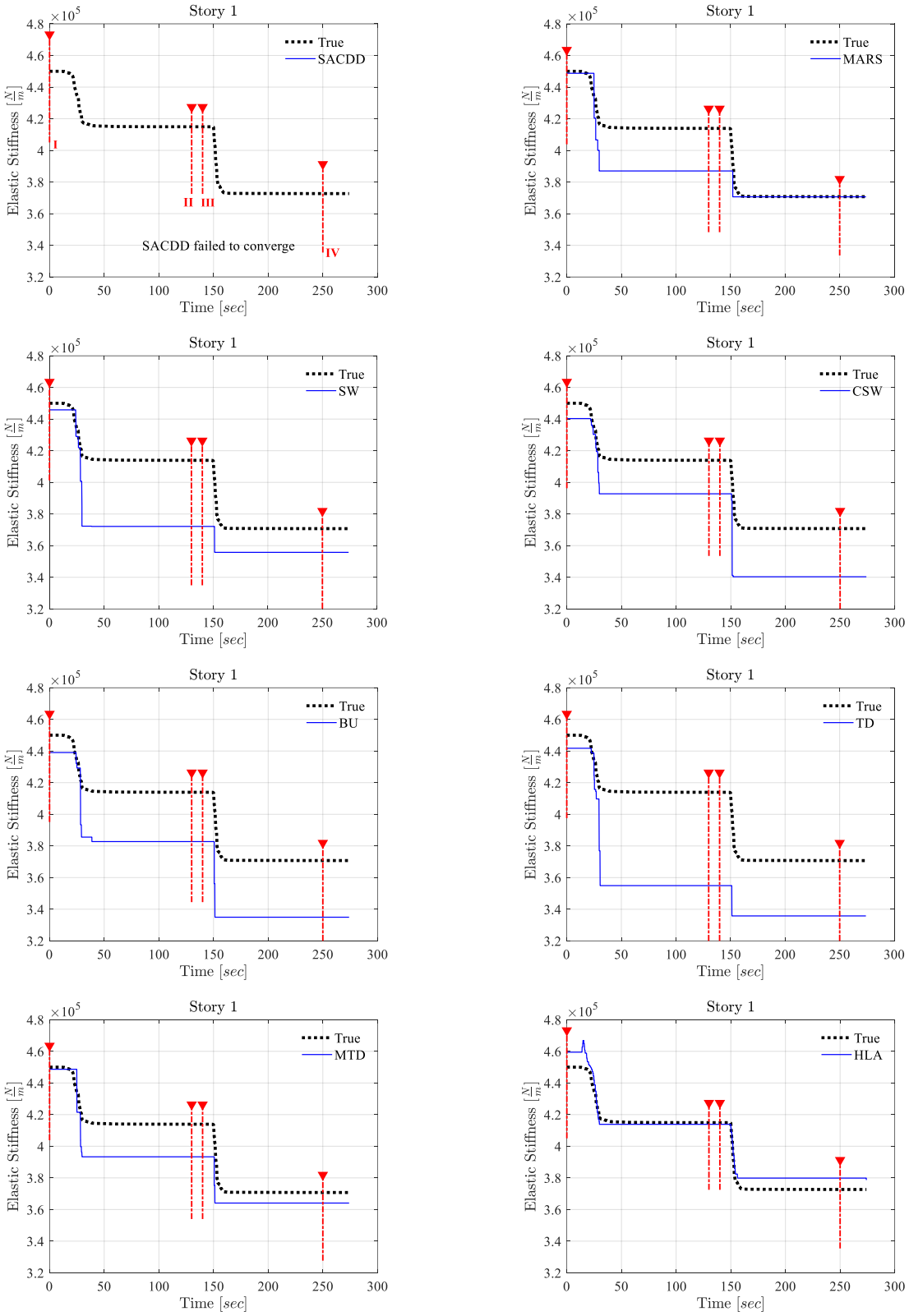

Fig. 4 – Estimated elastic stiffness of the first story for each method (Noise = 10% and sampling rate = 250 Hz).

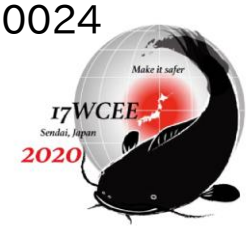

Fig. 4 compares the performance of HLA with the other methods in estimating the trajectory of elastic stiffness for the first floor in the noisy condition. Apart from SACDD failing, the identified stiffnesses at Stages II and III are almost equal for all methods. MARS is successful at Stages I and IV, but the error of these methods is significant in the middle stages, though errors at Stage I are smaller compared to Stages II, III, and IV. Moreover, MARS and MTD worked slightly better than HLA at Stage I, but not enough to ensure better accuracy later or to be meaningful in decision-making, as Stage I is the before event value.

According to the results, SACDD was the most unreliable method for SHM in this highly nonlinear structure with pinching behavior. SACDD is a model-based SHM technique [22]. Although model-based methods have been studied widely in civil engineering, selecting a suitable baseline model has remained a crucial issue. Model-based methods usually perform successfully only if the employed numerical model matches actual structure responses [9, 10, 16].

Thus, model-free SHM algorithms can have significant advantages over traditional model-based techniques, particularly in highly nonlinear cases like pinching behaviors. SW, CSW, BU, TD, and MTD are all model-free piecewise linear representation (PLR) algorithms [26]. They are supervised segmenting processes, where users are always required to tune some parameters, usually an error threshold [26, 27]. In SW, CSW, BU, and TD, the standard error $SE = 10$ is set. More optimal values may exist for any given case, but determining them requires human input and external knowledge for each structure, so they are not general or automated; and their accuracy is too sensitive to the level of sensor noise.

MTD is the modified version of TD. However, there are three thresholds to tune in MTD. The R^2 threshold helps the algorithm to avoid overfitting issues in small half-cycles. Second, the maximum number of linear segments required for representing each half-cycle must be defined for MTD, usually by observing the shape of hysteresis loops, thus requiring human input. Third, the minimum sample length of a segment is set to 3. These modifications made MTD more robust to sampling rate and noise compared to the other PLR algorithms. However, again, these values are based on human input and render the algorithm less general.

In MARS, no parameters need to be adjusted by the user. All breakpoints and linear segments are determined automatically [23-25]. However, results show MARS could not match HLA in identifying elastic stiffness. Hence, though MARS can be general, it lacks accuracy.

HLA requires no human inputs and determines the evolution of elastic stiffness over time from the measured responses automatically. Results show HLA is very robust to sampling rate and sensor noise. Although the sampling rate influence on the HLA accuracy is investigated for the first time in this paper, HLA performance for noisy and real-world conditions has been proven numerically and experimentally [9, 12-16].

A single test structure with a full range of nonlinearity should be employed to test the robustness of the methods and validate these simulated-based results over all methods. HLA is already well-proven for full-scale and scaled test structures on several studies [9, 12, 14, 16]. Thus, its generalisability is known. In this paper, the simulated case study highlights its relative capability and its significant robustness across a range of sampling rates in particular.

5. Conclusions

In this paper, one model-based SHM method and six model-free methods are employed for challenging the model-free HLA method to identify elastic stiffness evolution. For this purpose, a simulated highly nonlinear pinched hysteretic structure is subjected to two major earthquakes to investigate their robustness, consistency and accuracy. Identified stiffness values are compared to simulated known ground-truth values at four selected Stages (I-IV) across two events for each method. The impact of sampling rate and sensor noise on accuracy are assessed. The conclusions are summarised:

- HLA was robust to sampling rate with little change in accuracy. All other methods declined in accuracy with lower sampling rate. These are best case results without noise to independently assess the effect of sampling rate.

- HLA was equally to more accurate in the presence of noise, particularly when avoiding maximum errors, which might impact decision-making. It was the most accurate method through Stages I-II when assessing damage. The overall results for all methods highlight the robustness of model-free methods and also show how methods can vary significantly despite similarities.
- HLA is implemented in an automated function requiring no professional or engineering input, while all model-free PLR-based methods used here need a priori knowledge and human input to tune optimal thresholds for good accuracy.

6. References

[1] Doebling SW, Farrar CR,Prime MB (1998): A summary review of vibration-based damage identification methods. *Shock and vibration digest*, **30** (2), 91-105.

[2] Jin S-S, Cho S,Jung H-J (2015): Adaptive reference updating for vibration-based structural health monitoring under varying environmental conditions. *Computers & Structures*, **158** 211-224.

[3] Huang XH, Dyke S, Sun Z,Xu ZD (2017): Simultaneous identification of stiffness, mass, and damping using an on-line model updating approach. *Structural Control and Health Monitoring*, **24** (4), e1892.

[4] Ou G, Dyke SJ,Prakash A (2017): Real time hybrid simulation with online model updating: An analysis of accuracy. *Mechanical Systems and Signal Processing*, **84** 223-240.

[5] Chase JG, Hwang KL, Barroso LR,Mander JB (2005): A simple LMS-based approach to the structural health monitoring benchmark problem. *Earthquake engineering & structural dynamics*, **34** (6), 575-594.

[6] Chase JG, Spieth HA, Blome CF,Mander J (2005): LMS-based structural health monitoring of a non-linear rocking structure. *Earthquake engineering & structural dynamics*, **34** (8), 909-930.

[7] Chase JG, Begoc V,Barroso LR (2005): Efficient structural health monitoring for a benchmark structure using adaptive RLS filters. *Computers & structures*, **83** (8-9), 639-647.

[8] Nayyerloo M, Chase J, MacRae G,Chen X (2011): LMS-based approach to structural health monitoring of nonlinear hysteretic structures. *Structural Health Monitoring*, **10** (4), 429-444.

[9] Zhou C, Chase JG, Rodgers GW,Xu C (2017): Comparing model-based adaptive LMS filters and a model-free hysteresis loop analysis method for structural health monitoring. *Mechanical Systems and Signal Processing*, **84** 384-398.

[10] Xu C, Chase JG, Rodgers GW,Zhou C (2014): Multi-Phase Linear Regression: A Novel Method for the Identification of Base-Isolated Buildings Using Seismic Response Data. *Eurodyn 2014: Ix International Conference on Structural Dynamics*.2599-2604.

[11] Zhou C, Chase JG, Rodgers GW, Tomlinson H,Xu C (2015): Physical parameter identification of structural systems with hysteretic pinching. *Computer-Aided Civil and Infrastructure Engineering*, **30** (4), 247-262.

[12] Zhou C, Chase JG, Rodgers GW, Huang BF,Xu C (2017): Effective Stiffness Identification for Structural Health Monitoring of Reinforced Concrete Building using Hysteresis Loop Analysis. *X International Conference on Structural Dynamics (Eurodyn 2017)*, **199** 1074-1079.

[13] Zhou C, Chase JG, Rodgers GW,Iihoshi C (2017): Damage assessment by stiffness identification for a full-scale three-story steel moment resisting frame building subjected to a sequence of earthquake excitations. *Bulletin of Earthquake Engineering*, **15** (12), 5393-5412.

[14] Zhou C, Chase JG,Rodgers G (2017): Efficient hysteresis loop analysis-based damage identification of a reinforced concrete frame structure over multiple events. *Journal of Civil Structural Health Monitoring*, **7** (4), 541-556.

[15] Zhou C (2016): Efficient hysteresis loop analysis based structural health monitoring of civil structures. PhD Thesis Mechanical Engineering, University of Canterbury, Christchurch, New Zealand.

[16] Zhou C, Chase JG,Rodgers GW (2019): Degradation evaluation of lateral story stiffness using HLA-based deep learning networks. *Advanced Engineering Informatics*, **39** 259-268.

[17] Clifton C, Bruneau M, MacRae G, Leon R,Fussell A (2011): Steel structures damage from the Christchurch earthquake series of 2010 and 2011. *Bulletin of the New Zealand Society for Earthquake Engineering*, **44** (4), 297-318.

[18] Cifuentes AO,Iwan WD (1989): Nonlinear system identification based on modelling of restoring force behaviour. *Soil dynamics and earthquake engineering*, **8** (1), 2-8.

[19] Stephens JE,Yao JT (1987): Damage assessment using response measurements. *Journal of Structural Engineering*, **113** (4), 787-801.

[20] Toussi S,Yao JT (1983): Hysteresis identification of existing structures. *Journal of Engineering Mechanics*, **109** (5), 1189-1202.

[21] Xu C, Chase JG,Rodgers GW (2015): Nonlinear regression based health monitoring of hysteretic structures under seismic excitation. *Shock and Vibration*.

[22] Amini F,Rabiepour M (2017): A novel online damage detection approach in bilinear chain-like structures. *Journal of Civil Structural Health Monitoring*, **7** (2), 245-261.

[23] Friedman J (1993): Fast MARS. *Technical Report No. 10*, Department of Statistics, Stanford University, USA.

[24] Friedman JH (1991): Multivariate Adaptive Regression Splines. *Annals of Statistics*, **19** (1), 1-67.

[25] Hastie T, Tibshirani R, Friedman J,Franklin J (2005): The elements of statistical learning: data mining, inference and prediction. *The Mathematical Intelligencer*, **27** (2), 83-85.

[26] Keogh E, Chu S, Hart D,Pazzani M (2001): An Online algorithm for segmenting time series. *2001 Ieee International Conference on Data Mining, Proceedings*.289-296.

[27] Salvador S,Chan P (2004): Determining the number of clusters/segments in hierarchical clustering/segmentation algorithms. *Ictai 2004: 16th Ieee Internationalconference on Tools with Artificial Intelligence, Proceedings*.576-584.

[28] Baber TT,Noori MN (1985): Random Vibration of Degrading, Pinching Systems. *Journal of Engineering Mechanics-Asce*, **111** (8), 1010-1026.

[29] Baber TT,Noori MN (1986): Modeling General Hysteresis Behavior and Random Vibration Application. *Journal of Vibration Acoustics Stress and Reliability in Design-Transactions of the Asme*, **108** (4), 411-420.

[30] Pelliciari M, Marano GC, Cuoghi T, Briseghella B, Lavorato D,Tarantino AM (2018): Parameter identification of degrading and pinched hysteretic systems using a modified Bouc–Wen model. *Structure and Infrastructure Engineering*, **14** (12), 1573-1585.

[31] Sues R, Mau S,Wen Y-K (1988): Systems identification of degrading hysteretic restoring forces. *Journal of Engineering Mechanics*, **114** (5), 833-846.

[32] Bradley BA,Cubrinovski M (2011): Near-source Strong Ground Motions Observed in the 22 February 2011 Christchurch Earthquake. *Seismological Research Letters*, **82** (6), 853-865.

[33] Bradley BA, Quigley MC, Van Dissen RJ,Litchfield NJ (2014): Ground Motion and Seismic Source Aspects of the Canterbury Earthquake Sequence. *Earthquake Spectra*, **30** (1), 1-15.

[34] Milborrow S (2011): earth: Multivariate Adaptive Regression Splines, R package.

[35] Moghaddasi M, Cubrinovski M, Chase JG, Pampanin S,Carr A (2011): Effects of soil-foundation-structure interaction on seismic structural response via robust Monte Carlo simulation. *Engineering Structures*, **33** (4), 1338-1347.

